The Color of Glass

Georges Calas, Laurence Galoisy, Laurent Cormier

6.2

The Color of Glass

Georges Calas, Laurence Galoisy, and Laurent Cormier

Institut de Minéralogie, de Physique des Matériaux et de Cosmochimie, Sorbonne Université - CNRS - IRD - MNHN, Paris, France

1 Introduction

Color has been a most attractive feature of glass for millenia, from the glazes and pearls of the Suse period (4000 BCE) to the elaborated Roman houseware at the beginning of our era and to the stained glasses that blossomed during the European Middle-Ages. The kaleidoscope represented by medieval stained glasses (Figures VI and 1) illustrates the wide range of coloration of these glasses. The analysis of the coloration mechanisms gives information on the elaboration conditions, redox, and fining conditions.

The control of color throughout the synthesis process is a key component of glassmaking. This importance was underlined by Weyl's founding book, "*Colored glasses*," where much of the knowledge on this topic available in the 1950s was summarized [1]. In present-day technology, functional glasses are often developed because absorption bands within UV and IR regions give rise to specific applications. This is, for instance, the case of iron-bearing glasses for which the main absorption band of Fe^{2+} in the 1000–1200 nm region makes efficient absorption of solar energy possible, while keeping light transmission in the visible range sufficient to ensure adequate visibility through car windshields. On a more general basis, the limited energy range in which oxide glasses are absorbing, because of the presence of (un)wanted impurities, does not preclude these glasses to be commonly transparent in the near-IR (Chapter 6.1), which is an important parameter for modeling the diffusive radiative transport.

The color of a glass depends on light absorption, scattering, or reflection at wavelengths in the immediate vicinity of the visible spectral region. As other coloration processes, it depends also on the incident light source used and on the observer's eye sensitivity. In the absence of coloring agents such as chemical impurities, defects, clusters, and nanophases, most oxide glasses are colorless because they do not absorb visible light. This is the very reason for their extensive use as components for optical instruments or communications, e.g. silica glass for light transmission down to 160 nm, beyond the transmission domain of the Earth's atmosphere.

In the presence of impurities or structural defects, glasses are colored by selective absorption in specific regions of the visible spectrum. Optical absorption then gives indications on the nature and structural environment of coloring species and, in turn, on glassmaking parameters such as batch composition, furnace atmosphere, melting temperature, or duration of the melting process. Glass color is an exemplary illustration of structure–property relationships in glasses [2] through the connection between the atomic-scale structure of the glass and the nature and the intensity of the absorption bands that cause glass coloration. As will now be shown, the physical mechanisms behind coloration can be ligand-field effects, charge-transfer processes, or quantum-confinement effects in metal or semiconductor nanoparticles.

2 Background on Color Processes

2.1 Light Transmission by Glasses

The color of glass arises from variations in the light transmission efficiency throughout the visible spectrum, which lies between about 400 and 800 nm (Chapter 6.1). At the origin of coloration are absorption bands or

Reviewers: P. Bingham, Sheffield Hallam University, Sheffield, UK
M.-H. Chopinet, Saint-Gobain Recherche, Aubervilliers, France

Encyclopedia of Glass Science, Technology, History, and Culture, First Edition. Pascal Richet.

absorption edges whose effects are measured in terms of light transmission T through a glass plate

$$T = I/I_0, \tag{1}$$

(a)

(b)

Figure 1 French stained glass from the thirteenth century (cf. Figure VI). (a) Notre-Dame of Chartres cathedral (1215–1240), Bay 5, James and Josuas, detail of The life of St. James the Greater (cf. Figure VI), Chartres. © Malnoury, Robert; Martin, J., Inventaire général, ADAGP. (b) Sainte 694 Chapelle, Paris (1245–1250). © RMN (Musée de Cluny, Paris). (See electronic version for color figures)

where I_0 and I represent the intensities of the incident and transmitted light, respectively. Reflection losses occur at glass–air interfaces, however, but they are readily accounted for because the intensity of the incident (I_{in}) and reflected ($I_{\text{Reflected}}$) beams are related by

$$I_{\text{Reflected}} = I_{\text{in}}\,(n-1)^2/(n+1)^2, \tag{2}$$

where n is the index of refraction of the glass. For a soda-lime-silica glass ($n = 1.523$), Eq. (2) indicates that a fraction f of approximately 0.04 of the incident beam is reflected at each interface, regardless of the wavelength in the visible region where n varies by about 0.01.

Because light absorption depends on both glass thickness (l) and concentration of coloring elements (c), a more fruitful assessment of the process relies on Beer–Lambert law, which relates for a given wavenumber the absorbance A to these parameters and to the molar absorption coefficient ε (also known as molar extinction coefficient, or molar absorptivity)

$$A = \log\,(I_0/I) = \log\,(1/T) = \varepsilon c l. \tag{3}$$

The ratio A/l is referred to as the linear absorbance, allowing comparison between samples with different thicknesses. As indicated by Eq. (3), the transmission as a function of wavelength and absorbance as a function of wavenumber are easily interconverted. For a soda-lime glass, however, the two representations do not carry the same information in the visible and near-infrared spectral regions (Figure 2). Whereas transmission is the property of interest in practical applications, the absorption spectrum has to be considered instead in order to understand the coloration mechanisms because its bands can be assigned to definite structural components. Transmission to absorbance interconversion is probably one among the most spectacular structure–property relationships in materials.

At short wavelengths (or high wavenumbers), one observes the onset of UV absorption, which is due to electronic transitions between the valence and conduction band tails across the bandgap. This absorption edge can be described by another absorption coefficient, α, which follows an exponential Urbach-type law as a function of the wavenumber ν,

$$\alpha \sim \exp\,(h\nu/E_{\text{u}}), \tag{4}$$

where E_{u} is the Urbach energy that accounts for the energy distribution of the localized states in the valence band tail. On this absorption edge are superimposed intense charge-transfer bands, also located in the near UV, which have a Gaussian lineshape (see Section 5).

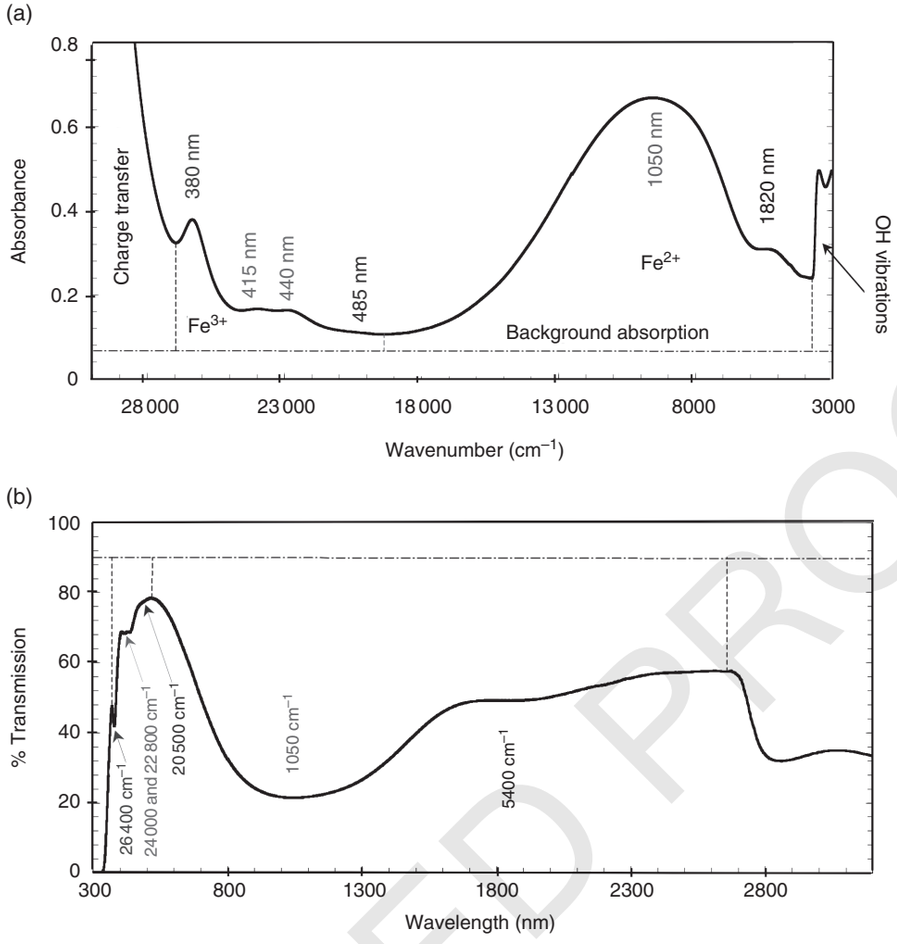

Figure 2 Glass coloration as examined from the standpoints of absorption and transmission for a soda-lime silicate glass containing 0.87 wt % Fe_2O_3 (sample thickness 4 mm). In the absorbance spectrum (a), the electronic transitions of Fe^{2+} and Fe^{3+} are clearly apparent in the near IR and visible-near UV, respectively. As to the transmission spectrum (b), it is used to represent coloration and provides colorimetric parameters. *Source:* After [3]. (See electronic version for color figures)

2.2 The Role of Transition Elements as Coloring Agents

The color of glass is generally due to electronic transitions in transition elements between localized electronic energy levels that are split by the ligand field. Transition elements are characterized by the presence of unpaired electrons in partially filled d- or f-orbitals. Electronic transitions within these orbitals are at the origin of selective light absorption at characteristic energies, usually within or in the vicinity of the visible spectrum [4]. The energy and intensity of these transitions vary as a function of the transition metal ion present, its oxidation state, and its immediate surrounding (site symmetry, nature of the ligands).

As d–d transitions are parity forbidden according to the selection rules for electric dipole transitions (Laporte rule), transition elements in principle should not have a high coloring efficiency. This feature holds particularly true for 4f-elements, in which the electronic levels retain an atomic character because 4f-orbitals are shielded by the outer electronic shells and not admixed with other electronic states. Hence, the molar absorption coefficient of lanthanides is 5–10 times smaller than that of 3d elements, yielding only faint colors even at concentration levels of several wt %.

For d-transition elements, the d-orbitals are not shielded by outer orbitals so that there is some admixture with other states when there is no inversion center at the site occupied by the transition element (distorted sites, tetrahedral or 5-coordinated sites). This admixing partially relaxes the Laporte selection rules, making 3d-elements such as Fe, Cu, Cr, V, Mn, Co, and Ni the major

coloring agents in glasses. Two main mechanisms are involved: (i) electronic transitions between crystal-field split 3d-electronic levels; (ii) charge-transfer processes, i.e. a transfer of the electronic density between the transition element ion and its ligands or other neighboring transition elements. As compared with the former, the latter is allowed and then results in an intense coloration. In both cases, optical transitions depend on the speciation of the transition element, namely its oxidation state, coordination number, site distortion, and on the nature of the chemical bond with its ligands (Table 1).

2.3 The Sites Occupied by Transition Elements in Glasses: A Limited Disorder

The fact that glass coloration can be assigned to one or several species of transition elements indicates the presence of well-defined cation sites. It is thus an obvious inadequacy of the Zachariasen model of oxide glasses not to describe the local environment of cations. During the last decades, many experimental studies and numerical simulations have demonstrated that the structure of oxide glasses and melts is more organized than assumed with a continuous random network. They have shown that cations are not restricted to fill holes within the polymeric network but tend to define their own environment according to the well-known crystal-chemical rules that exist in crystals. A major advance has thus been this conclusion that cations have a heterogeneous structural distribution, which contributes to an original medium-range order of oxide glasses and makes it possible to explain charge-transfer processes involving transition elements.

Because of a usually lower density caused by atomic disorder, the coordination number of cations is generally lower in glasses than in crystals of similar composition. Some cations mimic network formers by occurring in tetrahedra connected to the polymeric network within a well-defined topology: such are the cases of tetrahedral Ni^{2+}, Zn^{2+}, and Fe^{3+}. Network modifiers are cations such as alkalis or alkaline earths that are 6- or higher-coordinated. Contrary to what is observed in crystals, however, few transition metal ions are octahedrally coordinated in glasses and there is no evidence for higher coordination of 3d ions. The most important ions adopting an octahedral coordination are trivalent and highly charged cations such as Cr^{3+}, V^{3+}, or Zr^{4+}, as well as Co^{2+} and Ni^{2+} in the special case of alkali-poor borate glasses where they occur as CoO- and NiO-derived 2D-nanodomains.

Other transition metal ions such as Fe^{2+}, Ni^{2+}, and Fe^{3+} are frequently distributed among various site geometries whose proportions and resulting effects on color depend on chemical composition. They are often 5-coordinated – a coordination seldom observed in crystals – which gives rise to original colorations. This structural evidence points to the presence of small sites where cations have a structural role intermediate between those of network formers and modifiers. But the fact that transition metal ions cause well-defined optical absorption spectra in glasses indicates that their site distribution is limited despite the amorphous structure of these materials. The need for satisfying the charge neutrality of ligands implies a connection to the glassy polymeric network and indicates that a concept of quasi-molecular complexes does not describe the actual structural location of these ions.

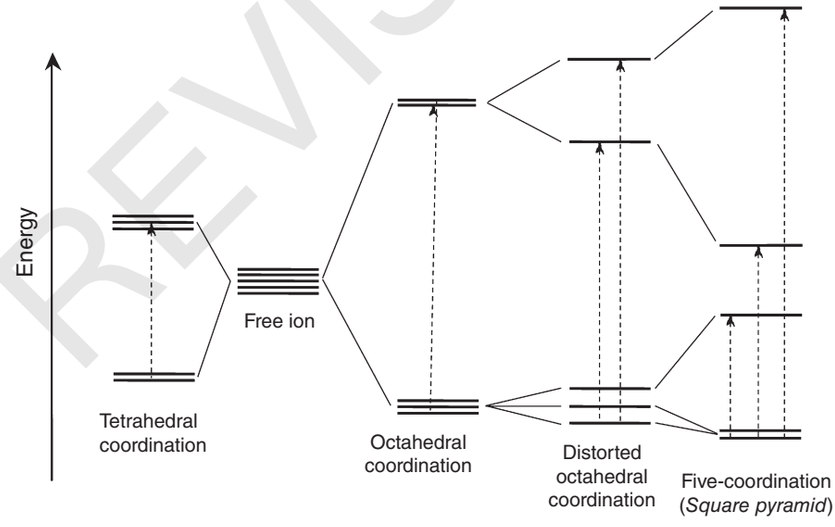

Figure 3 Successive splittings of d-orbitals of transition elements in different coordination numbers and site geometry. The dashed lines represent the electronic transitions that can be observed in a one-electron system.

3 Crystal-Field-Driven Glass Color

3.1 Crystal-Field Effects

The relative energy of d-orbitals varies as a function of the coordination number and distortion of the site occupied by the transition element, and by the bond covalency with the ligands. All these factors give rise to characteristic splittings (Figure 3) that make transitions between these electronic levels possible with a selective absorption of light that causes glass coloration. The position of these electronic levels gives indications on the local symmetry and magnitude of the ligand field splitting.

The intensity of these transitions is determined by selection rules for which the spin state of the transition metal ions plays an important role since absorption bands are less intense when the transition implies a change of the electron spin. For instance, Mn^{2+} and Fe^{3+} are not efficient coloring agents because both ions have five electrons occupying the five d-orbitals (Figure 4a), which leaves room for only spin-forbidden transitions of low intensity. Although less abundant than Fe^{3+} in glasses melted in air, Fe^{2+} gives them their characteristic green coloration caused by the presence of an intense absorption band in the near-infrared because a sixth 3d-electron (Figure 4a) produces spin-allowed electronic transitions. This contrast is reflected in the molar absorption coefficient of these ions, which is an order of magnitude lower for Fe^{3+} relative to Fe^{2+} (Figure 4b). Molar extinction

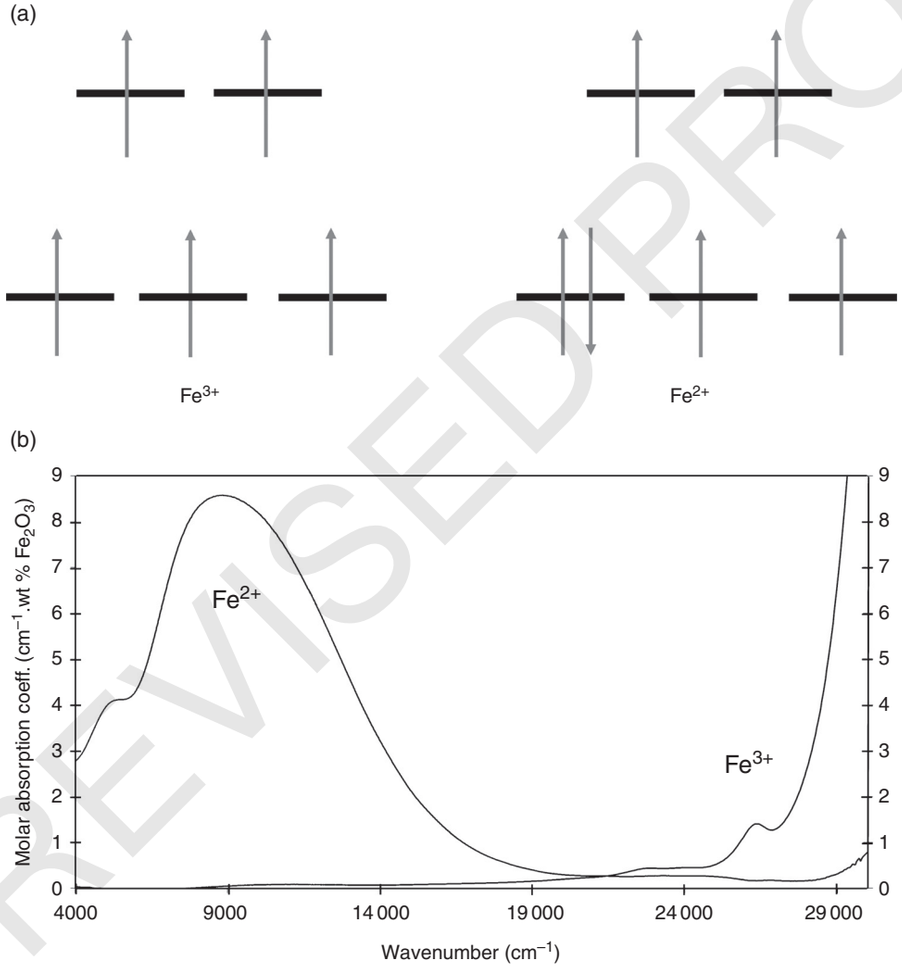

Figure 4 Influence of the electronic configuration on the optical absorption efficiency of Fe^{2+} and Fe^{3+}. (a) Schematic representation of the population of 3d orbitals. For Fe^{3+}, five electrons occupy the five d-orbitals so that d–d transitions are forbidden. For Fe^{2+}, the sixth electron gives rise to an electronic transition. (b) Spectral dependence of the molar absorption coefficient of Fe^{3+} and Fe^{2+} in a soda-lime-silica glass. *Source:* After [3]. The large difference in coloring power between these oxidation states results from the different electronic configuration shown in (a).

coefficients are important to model optical absorption spectra in glasses, provided the chemical composition of the glasses be similar: as optical properties are additive, it is possible to compute optical absorption spectrum expected from the presence of various coloring elements (Table 2).

Finally, another factor to be taken into account is the electrostatic repulsion between 3d-electrons because it influences the optical absorption spectra by shifting the free-ion electron energy levels prior to the action of crystal field. This interelectronic repulsion can be expressed in terms of three parameters A, B, and C known as the Racah parameters (after Giulio Racah, who first described them). Racah parameters are ion-specific and for a given ion vary with the electron localization (i.e. with cation-ligand bond covalency). The reduction of interelectronic repulsion between the 3d-electrons corresponds to a more covalent character of the transition metal ion oxygen bond.

3.2 Peculiar Sites, Peculiar Colors: The Example of Ni^{2+}

Nickel yields colors ranging from brown and yellow in Na-, Li-, or Ca-bearing glasses to purple or blue in K-, Rb-, or Cs-bearing glasses or, less commonly, green or even orange in some alkali-deficient borate and borosilicate glasses (Figure 5). This broad palette of hues in oxide glasses is directly related to the varying coordination of Ni^{2+} [6]. Probably one of the most commonly observed colors, the brown arises from continuously decreasing absorption from the purple to the red parts of the visible domain along with the absence of an absorption maximum in the visible domain. That color is indeed very sensitive to local structure as shown by a comparison between the optical absorption spectra of crystalline and glassy $CaO{\cdot}NiO{\cdot}2SiO_2$ (Figure 6). The former has the light green color characteristic of $^{[6]}Ni^{2+}$. In the latter, Ni^{2+} occupies a small proportion of tetrahedral sites but it is mostly present in triangular bipyramids that give rise to the brown color through a broad, asymmetric absorption band around 22 500 cm^{-1} (444 nm). Weak and broad absorption bands in the visible and near-infrared correspond to the other electric transitions expected for $^{[5]}Ni$. The existence of these $^{[5]}Ni$ sites has been confirmed by complementary Ni K-edge extended X-ray absorption fine structure (EXAFS) and X-ray absorption near edge structure (XANES) spectroscopy and neutron diffraction coupled with isotopic substitution. As underlined below for Fe^{2+}, however, most methods do not

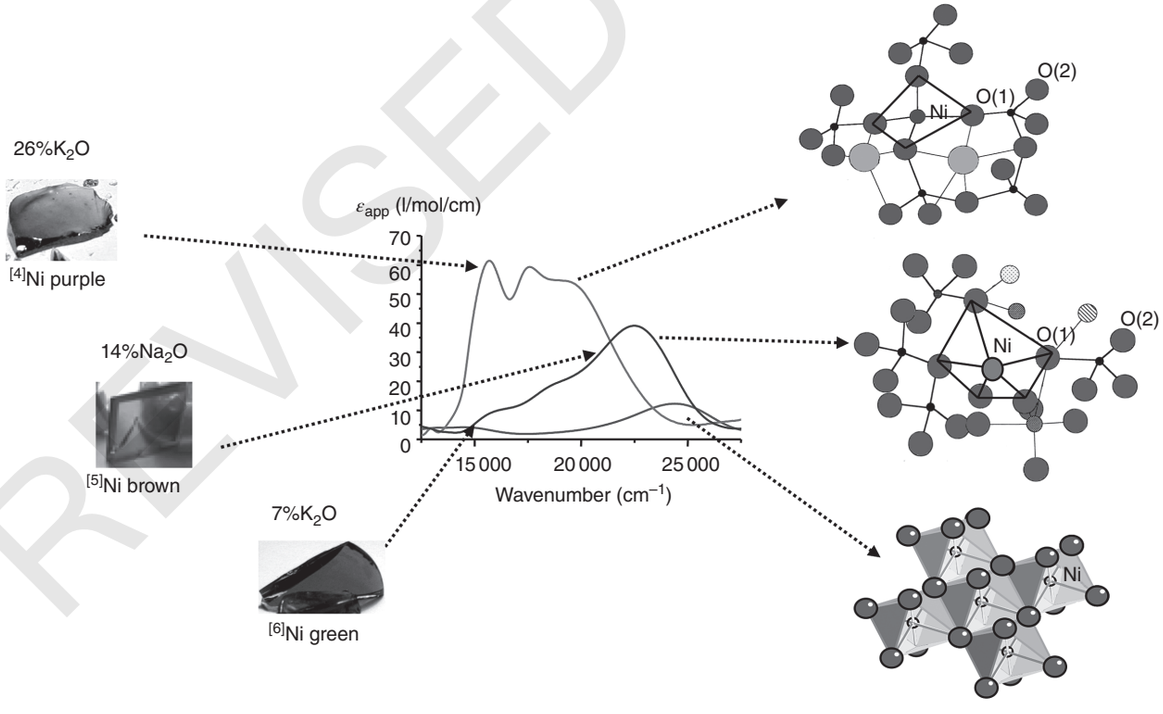

Figure 5 Optical spectra and structural models explaining the color of purple, brown, and green borosilicate glasses containing Ni^{2+} in four-, five-, and sixfold coordination, respectively. *Source:* After [5]. (*See electronic version for color figures.*)

provide indication on the actual site geometry of the $^{[5]}$Ni site, which has been mostly derived from optical absorption spectroscopy.

Optical transitions from tetrahedral Ni^{2+} are present as a minority contribution in most optical absorption spectra of Ni-bearing silicate, aluminosilicate, and borosilicate glasses, with the noticeable exception of low-alkali borate or borosilicate compositions. In glasses containing large alkalis (K, Rb, Cs), $^{[4]}Ni^{2+}$ causes a blue/purple coloration through the presence of an intense absorption band located near 16 000 cm^{-1}, in the red region of the visible spectrum, and a transmission window at short wavelengths (Figure 5). This chemical dependence of glass coloration will be discussed in Sections 4.1 and 6.1.

3.3 Peculiar Sites with a Continuous Site Distribution: Fe^{2+} and Fe^{3+}

Although iron is the most common coloring element in glasses, the geometry of the sites occupied by Fe^{2+} and Fe^{3+} is still a matter of debate in spite of numerous studies made with a broad range of structural and spectroscopic methods that includes X-ray and neutron diffraction, Mössbauer spectroscopy, electron paramagnetic resonance, XANES and EXAFS, optical absorption, and luminescence (Tables 1 and 2).

Like for Ni^{2+}, there is no evidence for octahedral coordination of Fe^{2+} in silicate glasses, but the picture is less clear-cut for Fe^{3+}. The optical absorption spectrum of Fe^{2+} shows two absorption bands, the most intense near 9000 cm^{-1} with an extension to higher wavenumbers in the red region that also affects glass coloration. A significant absorption down to 16 000 cm^{-1}, i.e. outside the absorption domain of octahedral Fe^{2+} in crystals, indicates the presence of $^{[5]}$Fe. A detailed magnetic circular dichroism study has confirmed that the Fe^{2+} absorption band is mostly caused by four- and fivefold coordinated species [7]. This result agrees with Mössbauer and Fe K-edge XANES and EXAFS data, which indicate that Fe^{2+} coordination varies continuously from four- to

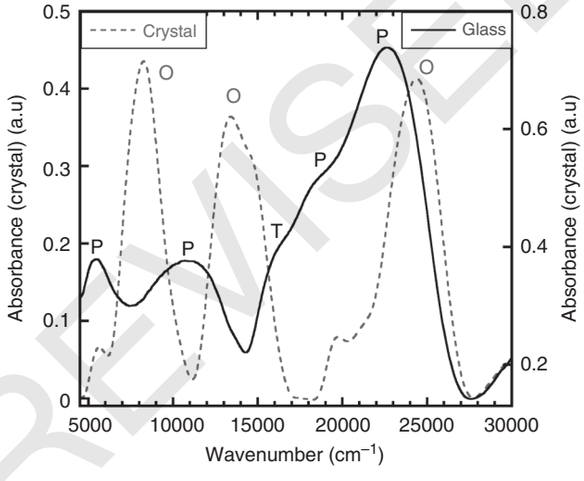

Figure 6 Effect of nickel coordination on the absorbance spectra (derived from diffuse reflectance) of $CaNiSi_2O_6$ crystal and glass which are green and brown, respectively. The position of the three similarly intense peaks of octahedral Ni^{2+} in the crystal (O) contrast with the two weak peaks and the large high-energy band produced by Ni^{2+} in the trigonal bipyramids of the glass (P), to which tetrahedral Ni^{2+} contributes a shoulder (T). *Source:* After [6]. (*See electronic version for color figures.*)

Table 1 Glass coloring mechanisms.

Cause of coloration	Examples	Efficient concentration
Crystal-field transitions	d-Elements	0.1–10 wt %[a]
Atomic-like transitions	4f-Elements	1–10 wt %
Ligand to metal charge transfer	O–Fe^{3+}, O–Ce^{4+}, S^{2-}–Fe^{3+}, O^{2-}–U(VI)	10–1000 ppm
Intervalence charge transfer	Fe^{2+}–Fe^{3+}, Fe^{2+}–Ti^{4+}	1–10 wt %
Nanoparticles	Au^0, AgCl, Cd(S, Se)	10–100 ppm

[a] Lower efficient concentrations for $^{[4]}Co^{2+}$ (some 10–100 ppm) and 4d- and 5d-elements (e.g. Pt^{4+}: a few 100 ppm).

Table 2 Color yielded by various transition metal ions in glasses.

Oxidation state	Coordination number	Color
Ti^{3+}	6 (distorted)	Lilac
V^{4+} (VO^{2+})	6 (distorted)	Blue
V^{3+}	6	Green
Cr^{VI} (CrO_4^{2-})	4	Yellow
Cr^{4+}	4	Blue
Cr^{3+}	6	Green
Cr^{2+}	6 (distorted)	Blue
Mn^{3+}	6 (distorted)	Purple
Mn^{2+}	4, 5	Light yellow/orange
Fe^{3+}	4, 5	Light yellow
Fe^{2+}	4, 5 (6?)	Green
Co^{2+}	4	Violet blue
Ni^{2+}	6	Apple green, yellow
Ni^{2+}	5	Brown
Ni^{2+}	4	Blue, purple
Cu^{2+}	6 (distorted)	Blue
Pt^{4+}	6	Yellow

fivefold. These complementary techniques do not provide further information on the actual site geometry of $^{[5]}$Fe sites, however, which may range from a square pyramid to a trigonal bipyramid geometry. Optical absorption spectra are very sensitive to this variation in the local symmetry that gives rise to distinct electronic transitions. A modification of the geometry of the $^{[5]}$Fe site as a function of glass composition may explain the variations observed in the position of the broad Fe^{2+} absorption band near 10 000 cm^{-1} in glasses. This continuous distribution thus contrasts with the bimodal distribution between discrete site geometries observed for Ni^{2+}, each one being characterized by well-defined spectroscopic parameters.

Owing to experimental difficulties, the interpretation of the Fe^{3+} optical absorption bands in glasses has also been much discussed. It nonetheless appears that (i) the most intense bands arise from field-independent transitions that do not depend on site geometry; (ii) the other crystal-field transitions are superimposed on and can be obscured by the tail of the intense O–Fe charge-transfer transitions that occur in the near UV; (iii) as underlined in Section 3.1, Fe^{3+} transitions are spin-forbidden and hence of lower intensities than those of Fe^{2+} by more than one order of magnitude. In a recent investigation of glasses in which iron was fully oxidized, however, Fe^{3+} speciation could be unambiguously determined by EXAFS [8]. Providing information on the origin of the transitions observed in the optical absorption spectra, this study clearly showed that Fe^{3+} coordination is changing from 4 to 6 as a function of the nature and concentration of the alkali and alkaline earth cations present, the coordination number of Fe^{3+} increasing with decreasing cation ionic radius ratio. Alkali–alkaline earth glasses show evidence of a stabilization of $^{[4]}Fe^{3+}$, illustrating a preferential link between $^{[4]}$Fe and the alkalis [8] and indicating that transition metal ions are not probing the average glass structure, but favor some local surroundings.

3.4 Presence of One Site Geometry: Cr^3

Like in most crystalline compounds, Cr^{3+} occurs in glasses only in octahedral coordination because of the high crystal-field stabilization energy of the d^3 configuration. The crystal-field spectrum of Cr^{3+} exhibits two broad, intense bands at 15 000 and 22 000 cm^{-1}, which occur in the visible range and have characteristic Gaussian line shapes with bandwidths close to that observed in crystals (Figure 7). This is consistent with the observed Cr–O interatomic distances and their small radial disorder determined by Cr K-edge EXAFS. These absorption bands define transmission windows near 10 000, 18 000, and 27 000 cm^{-1}: only the second one is responsible for the characteristic green color observed in Cr-bearing glasses since the others are outside the visible spectrum. Additional weak features near the maximum of the bands are linked to field-independent spin-forbidden transitions, resulting in characteristic interference dips.

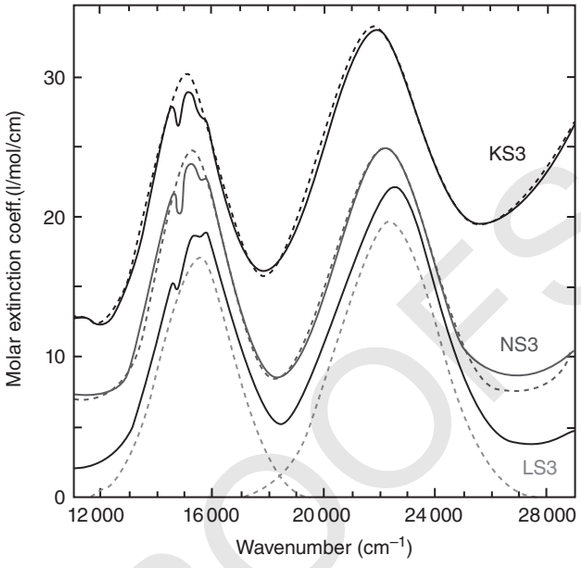

Figure 7 Molar extinction coefficients of Cr^{3+} in K-, Na-, and Li-trisilicate glasses (referred to as KS3, NS3, and LS3, respectively); experimental spectra (solid curves) and fits made with Gaussian bands (dashed curves), which are also plotted as dotted curves for LS3. For clarity, the data for NS3 and KS3 have been shifted upward by 2.7 and 12 L/mol/cm, respectively. *Source:* After [9]
(See electronic version for color figures.).

Other transition-element cations exhibiting only one site geometry in glasses include Ti^{3+}, V^{3+} and V(IV) (actually the vanadyl group, VO^{2+}), Cr^{2+} and Cr^{4+}, etc. Special mention must be made of Mn^{3+} and Cu^{2+} for which the main absorptions band undergo Jahn–Teller splitting of the excited e_g level through spontaneous distortion of the octahedral coordination, which increases the crystal-field stabilization energy. As a result, Mn^{3+} allows light transmission in the red and violet part of the visible spectrum, resulting in the characteristic pink/magenta color of Mn-bearing glasses, whereas Cu^{2+} exhibits a unique, large transmission window in the blue-green part of the spectrum.

3.5 The Case of Silent Species: Co^{2+}-Bearing Glasses

The typical blue color of Co-bearing glasses is due to an intense absorption band located in the orange and red parts of the visible spectrum that is characteristic of $^{[4]}Co^{2+}$ (Figure 8). This assignment from optical absorption spectroscopy is in agreement with XANES and EXAFS data. Even though the hue of Co-bearing glasses

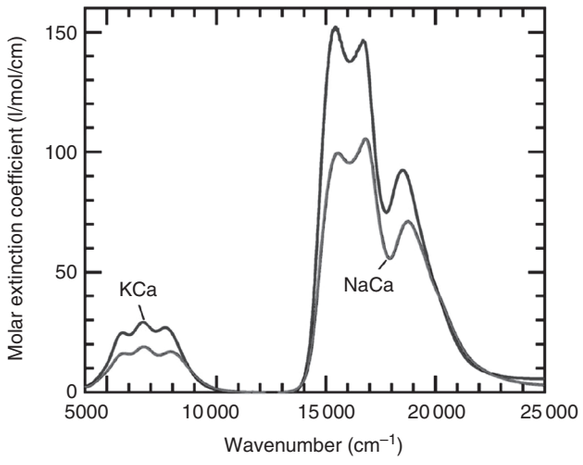

Figure 8 Influence of the nature of the alkali cation on the intensity but not on the lineshape of the optical absorption bands of Co^{2+}-bearing $K_2O{\cdot}CaO{\cdot}4SiO_2$ (blue) and $Na_2O{\cdot}CaO{\cdot}4SiO_2$ (red) glasses. Absorbance is represented as represented by the molar extinction coefficients, allowing quantitative comparison between the two glasses. *Source:* After [10]. (*See electronic version for color figures*.)

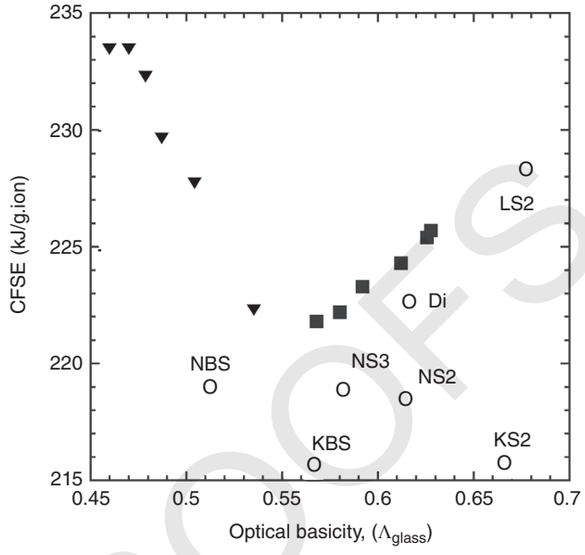

Figure 9 Variation of Cr^{3+} crystal-field splitting, represented as the crystal field stabilization energy (CFSE), as a function of optical basicity in glasses. Filled squares: multicomponent silicate and aluminosilicate glasses, which mimic chemical variations during magmatic differentiation; open circles: alkali silicate glasses (NS, KS, and LS refer to sodic, potassic, and lithic silicate glasses, respectively, NBS and KBS stand for sodium and potassium borosilicate glasses) and Di for diopside ($CaMgSi_2O_6$) glass; filled triangles: alkali borate glasses. *Source:* After [11].

does not vary much with glass composition, the intensity of the coloration (and hence of the absorption bands) does change. As an example, replacement of K by Na in $R_2O{\cdot}CaO{\cdot}4SiO_2$ (R = K, Na) glasses decreases the optical transition intensity by 35% whereas the molar extension coefficient of $^{[4]}Co^{2+}$ complexes is only half of the values reported for potassium and sodium silicate glasses. This is an indication that Co^{2+} converts to less absorbing, *silent* species when replacing a given alkali by either a smaller alkali or alkaline earths. As indicated by EXAFS data, the smaller molar extension coefficient cannot be attributed to a distortion of the Co tetrahedral site, as observed in crystals. These observations suggest the presence of higher coordinated, weakly absorbing species, that are difficult to quantify because the optical absorption bands of $^{[4]}Co^{2+}$ overlap the transitions expected for $^{[5]}Co^{2+}$ and $^{[6]}Co^{2+}$. Although the low intensity of these spectroscopically silent species does not help in recognizing them in optical absorption spectra, they directly affect the intensity of light absorption and hence the efficiency of Co^{2+} as a coloring agent.

4 Variation of Glass Coloration

4.1 Dependence of Color on Glass Composition

Changing glass composition affects the effective charge of the oxygen ligands, and hence crystal-field splitting magnitude as well as cation-oxygen covalence. Transition elements are indeed interesting structural probes of glass structure. Two different cases can be distinguished in this respect. When only one site geometry exists (e.g. Ti^{3+}, Mn^{3+}, Cr^{3+}, V^{4+}, and V^{3+}), the chemical dependence of the optical spectra manifests itself mostly through a shift of the main absorption bands. When two sites (e.g. Ni^{2+}, Ti^{4+}) or more (e.g. $^{[4]}Fe^{2+}$ and $^{[5]}Fe^{2+}$, $^{[8]}Nd^{3+}$ and $^{[9]}Nd^{3+}$) are present, their relative proportions vary with glass composition without much shifting of the electronic transitions. An abundant bibliography exists in this domain, but is mostly restricted to some specific glass systems. We will illustrate this section with Cr^{3+} and Ni^{2+}.

4.2 Variation of Site Geometry: Presence of a Single Type of Site

The case of Cr^{3+} has been studied extensively. This cation retains a regular octahedral coordination in most oxide glasses [11] in spite of some variations in the magnitude of crystal-field splitting and of disorder effects induced by glass composition mostly as a function of the nature of the modifier cation (but not of its concentration). In multicomponent glasses (Figure 9), the crystal-field intensity increases with optical basicity (cf. Chapter 5.7). In alkali silicate glasses, however, it varies only with the nature of the alkali and not with its concentration. In mixed

alkali–alkaline earth glasses, optical absorption parameters in addition remain close to the values found in binary silicate glasses with the same type of alkalis, which reveals that Cr^{3+} shows a strong preference for alkalis in its immediate environment. These observations indicate that Cr^{3+} is insensitive to the overall glass structure. It builds instead its own environment, which is also demonstrated by its heterogeneous distribution in the glass structure [11].

4.3 Variation of Site Geometry: Presence of Two Sites

When a glass bears an ion such as nickel that distributes between two sites, its color vary with glass composition [6] as the fractions of $^{[5]}Ni^{2+}$ and $^{[4]}Ni^{2+}$ sites. In silicate glasses, alkalis and alkaline earths are either network modifiers when they coexist with $^{[5]}Ni$ or charge-compensators for $^{[4]}Ni$. The mean Ni speciation thus depends only on the nature of the alkali or alkaline earth. As observed in Section 4.2 for 3d-ions in a single type of site, however, the concentration of the alkali or alkaline earth does not influence glass color in silicate glasses. By contrast, in borate and borosilicate glasses, the Ni-site geometry and color progressively change with increasing alkali or alkaline earth content from octahedral (green) to distorted octahedral (yellow), trigonal bipyramid (brown), and finally tetrahedral (purple). This trend likely arises from the interaction of alkali and alkaline earths with boron when its coordination changes from $^{[3]}B$ to $^{[4]}B$ with increasing alkali/alkaline earth concentration. As a consequence, some borosilicate glasses show a peculiar orange color that is otherwise rarely encountered. In this case, Ni has the three coordination numbers 6, 5, and 4: $^{[6]}Ni$ is probably associated with the borate sublattice, and $^{[5]}Ni$ and $^{[4]}Ni$ with the silicate sublattice.

4.4 Redox Equilibria and Glass Coloration

The influence of the redox state on glass color has been much investigated [12]. For instance, Cr-bearing glasses show a change in glass color from green to yellow when melting conditions vary from reducing to oxidizing. This trend is due to the formation of a chromate complex $(CrO_4)^{2-}$ that gives rise to a charge-transfer transition from oxygen to chromium located near 28 000 cm^{-1} in oxidized glasses (Figure 10). The tail of this intense band extends from the UV to the visible and is superimposed on the Cr^{3+} absorption bands because there exists a considerable difference between the molar extinction coefficients of Cr^{3+} and Cr^{6+}, which are 18–20 and 4200 l/(cm/mol), respectively. As a result, optical spectroscopy measurements of the chromium redox state cannot be made

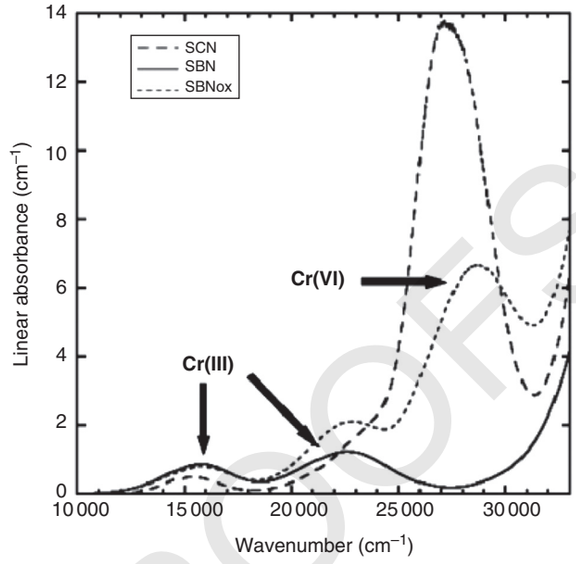

Figure 10 Linear absorbance spectra of Cr^{3+} and $(CrO_4)^{2-}$ in soda-lime-silica (SCN) and sodium borosilicate (SBN and SBNox) glasses. The position of the absorption bands characteristic of the two oxidation states of chromium in the glasses is indicated. *Source:* After [14].

on glasses in the presence of relatively high concentrations of Cr^{6+} in the form of chromate groups. Wet chemical analysis or other spectroscopic methods have to be performed instead.

The interaction between redox pairs is widely used during glass fining. For instance, manganese has traditionally been known as the *glassmaker's soap* because, if added to soda-lime-silica glass in the form of an oxide such as MnO_2, it makes the green color arising from iron impurities less intense by oxidizing Fe^{2+} into Fe^{3+}

$$Mn^{4+} + 2\,Fe^{2+} \rightarrow Mn^{2+} + 2\,Fe^{3+}.$$

And because only spin-forbidden transitions are associated with the d^5 configuration of both Mn^{2+} and Fe^{3+} (Figure 4a), their low intensities result in weakly colored glasses. The effect is not permanent, however, as the interaction with sunlight (solarization) favors the reverse reactions:

$$Mn^{2+} + h\nu \rightarrow Mn^{3+} + e^{-},$$

$$Fe^{3+} + e^{-} \rightarrow Fe^{2+}.$$

As illustrated by old windows and doorknobs, this phenomenon is at the origin of the well-known *purple glass* of which *desert amethyst glass* is a natural variety.

5 Temperature Dependence of the Optical Absorption Spectra of Glasses: Thermochromism

Color changes are often spectacular upon heating: brown Ni-bearing glasses, for instance, turn blue or green Cr^{3+}-bearing glasses into yellow (Figure 11). Like for the chemical dependence of glass coloration, there is a marked difference between transition elements depending on whether they occupy one or several sites. In the latter situation, temperature modifies the equilibrium between the site populations whereas in the former, the site of the coloring element expands with increasing temperature. Because of the difficulty of recording high-temperature optical absorption spectra, however, data are scarce so that we will restrict ourselves to discussing investigations made below T_g. We nonetheless warn that important modifications of the optical spectra may take place in the molten state.

5.1 Coexistence of Well-Defined Sites: Ni^{2+}

In a classic piece of work, Lin and Angell [15] investigated the optical absorption spectra of Ni^{2+} in a potassium triborate glass and melt to 1000 °C. In the starting glass, Ni^{2+} is distributed between 4- and 5-coordination as in most oxide glasses (see Section 3.1). Major changes occur in the vicinity of T_g, above which the proportion of $^{[4]}Ni^{2+}$ increases. This is likely related to the temperature-induced coordination changes of boron, as shown by the reaction

$$Na_{CC} + BO_4 \rightarrow BO_3 + O_{NBO} + Na_{NM} \quad (5)$$

where Na_{CC} and Na_{NM} stand for charge-compensating and network-modifying Na, respectively, and O_{NBO} for non-bridging oxygen. The $^{[4]}B$ to $^{[3]}B$ conversion between glass and melt increases alkali activity and then provides further charge compensation for $^{[4]}Ni$, inducing the coordination change of Ni. In the borate composition investigated, the $^{[4]}Ni/^{[5]}Ni$ ratio is not frozen in at T_g, as these two states are separated by unusually small energy barriers. The presence of further changes down to room temperature is a direct evidence of ionic mobility while the polymeric network is frozen in. The modification of Ni- and Co-speciation in glasses at high temperature may be retained after fast quenching. This has been recently shown in Co- and Ni-bearing alkali borosilicate glasses in which the 4-coordinated species, favored at high temperature, are partly retained at room temperature by a fast quenching, illustrating the importance of thermal history on glass structure [16].

5.2 Presence of One Site: Direct Evidence of a Thermal Expansion of Cation Sites

The crystal-field strength is a sensitive probe of the environment of transition elements in crystalline compounds and of its changes under high temperatures or pressures. High-temperature optical spectra of Cr^{3+} in glasses show a systematic linear redshift of the crystal-field transition from 300 to 800 K, with an isobestic point near 17 000 cm^{-1} (Figure 12). The transmission window similarly

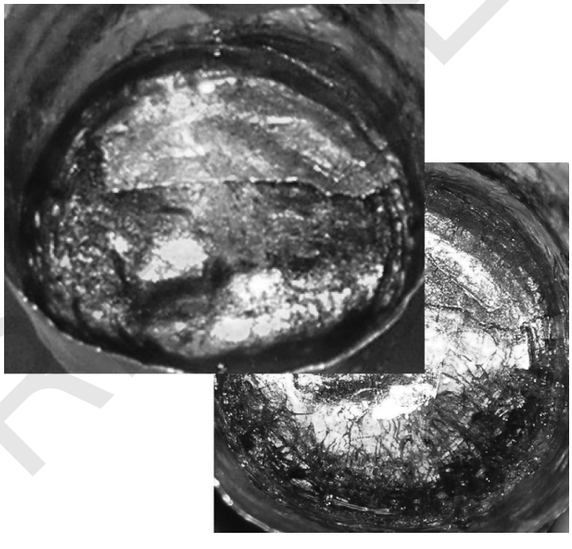

Figure 11 Green Cr-containing glasses turning yellow at ca. 500 °C, a direct illustration of the thermal expansion of cation sites in glasses. (See electronic version for color figures)

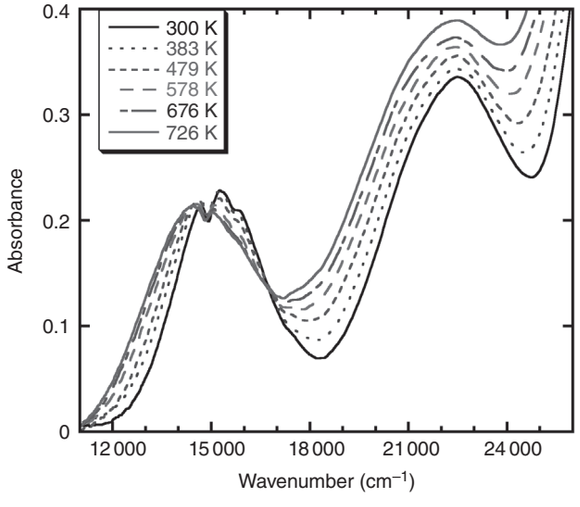

Figure 12 Modification of the optical absorption spectrum of Cr^{3+} in a potassium borosilicate glass from 300 to 726 K. *Source:* After [12]. (See electronic version for color figures)

shifts toward lower wavenumbers, giving glasses thermochromic properties [11]. Using a point charge model, one may derive the temperature-induced variation of the Cr–O distances from crystal-field splitting, Dq

$$10Dq = \frac{5q\langle r^4\rangle}{R^5} \quad (6)$$

where q is the effective charge in the ligands, r the d-electron-core distance, and $\overline{R}$ the mean Cr–O distance. In this way, one estimates the linear thermal expansion coefficients of Cr^{3+}–O bonds in glasses to be about $16–20{\cdot}10^{-6}$ K^{-1}. These values are independent on glass composition, contrary to what is observed for bulk thermal expansion, and they are in addition generally larger than the macroscopic thermal expansion coefficients. This lack of sensitivity of Cr^{3+} to the average glass structure is an additional confirmation of the heterogeneous structure of silicate glasses at the atomic scale [11]: Cr^{3+} does not explore an average glass structure but rather adjusts its own environment.

6 Charge-Transfer Processes: From (Amber Glasses to Lunar Glasses)

6.1 Ligand to Metal Charge Transfer (LMCT)

Charge transfer (CT) represents a shift of the electron charge density from one ion to a neighboring one. The most frequent processes involve transition metal ions such as Fe^{2+}, Fe^{3+}, Ti^{4+}, Ce^{3+}, Ce^{4+}, and their ligands (O, S, Se…) in relation with the covalency of the chemical bond. They give rise to intense absorption bands at short wavelengths, providing a strong UV absorption in glasses that would otherwise be mostly transparent in the visible range. These glasses are thus used for solar protection and they also ensure efficient UV absorption in food containers.

The reduction of glass transparency in the UV arises from the presence of Gaussian-shaped absorption bands, superimposed on an exponential Urbach absorption edge and related to the presence of ligand-to-metal CT transitions. The intensity of these bands is larger by about three orders of magnitude than that of crystal-field transitions. The O^{2-}–Fe^{3+} CT band near 45 000 cm^{-1} dominates the shape of the UV absorption edge [17], and may be detected at low concentration down to ppm levels. For Fe^{2+}, CT is about three times less intense and occurs at slightly higher energy than for Fe^{3+}. Likewise, Ce^{3+} and Ce^{4+} are strong UV absorbers in glasses where, as observed for iron, absorption is more efficient (by a factor of 16) and takes place at higher wavenumbers for the oxidized than for the reduced form [18]. Other transition metal ions show intense ligand-to-metal transitions in the UV, e.g. near 33 000 cm^{-1} for Ti^{4+} [19].

Increasing the covalency of Fe-ligand bond shifts the energy of the charge-transfer transition toward lower values. Such is the case of the well-known amber chromophore, which is widely used to efficiently absorb UV radiation and then protect radiation-sensitive liquids in glass containers (pharmaceuticals and beverages). This chromophore shows optical transition near 23 500 cm^{-1} with a molar extinction coefficient of about 9000 L/mol/cm (as compared to 25 L/mol/cm for the Fe^{2+} absorption band near 1000 nm). As a consequence, the amber chromophore contributes to glass coloration at concentrations as low as a few ppm: the high intensity of these bands causes them to extend into the visible spectrum. The continuously decreasing absorption from the violet to red gives rise to this characteristic brown coloration. The structure of this amber chromophore is still poorly known, involving $^{[4]}Fe^{3+}$ ions surrounded by one S^{2-} and three O^{2-} ions. Its stability field is then limited by two opposite redox reactions, i.e. the reduction of ferric iron and the oxidation of sulfide ligands.

A peculiar case concerns oxyanion and oxycation complexes such as chromate $(CrO_4)^{2-}$, vanadate $(VO_4)^{3-}$, or uranyl $(UO_2)^{2+}$ groups. Under oxidizing conditions, these complexes are similar in glasses to those observed in crystals and aqueous solutions, retaining similar spectral properties. As a d^0 system, the formal Cr(VI) or V(V) oxidation states do not have d electrons, so that the only electronic transitions occur via charge-transfer processes from ligands to the central ion, which is at the origin of the intense coloration arising from these extreme oxidation states. For instance, CT in chromate groups consists of a transfer of an oxygen p electron, constituting one of the ligand bonds of $t_1\pi$ symmetry, to the central ion d-shell. Further splitting by crystal field gives rise to two absorption bands near 37 000 and 27 000 cm^{-1} [20]. Only the latter is usually observed because the former is hidden by the absorption of the matrix (Figure 12).

6.2 Intervalence Charge Transfer

Another type of CT involves cations with different oxidation states, which also relies on an extended covalency of chemical bonds and give rise to absorption bands so intense that these may even result in efficient coloration at concentrations down to the ppm level. Increasing the iron content in oxide glasses, for instance, increases absorption in the visible region between ligand-to-metal CT in the near UV and crystal-field transitions in the near IR so that high-Fe glasses melted in air are black (Figure 13). Evidence has been found for a contribution near 14 500 cm^{-1}, assigned to Fe^{2+}–O^{2-}–Fe^{3+} intervalence charge transfer (IVCT), Fe^{2+} and Fe^{3+} playing the

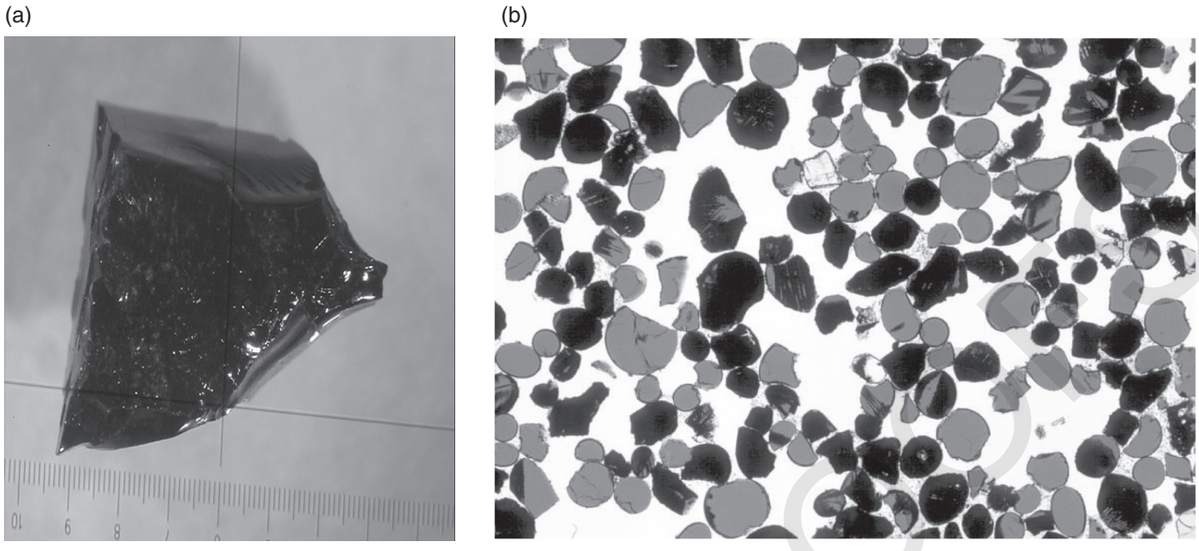

Figure 13 Coloration arising from charge transfer processes. (a) Dark color of $NaFeSi_2O_6$ glass (Fe^{2+}–Fe^{3+} intervalence charge transfer). (b) Orange glass ("soil") collected during the Apollo 17 mission. Clear orange beads owe their color to Fe^{2+}–Ti^{4+} intervalence charge transfer. The black color of some grains comes from the surface nucleation of olivine crystals with intergrown ilmenite ($FeTiO_3$) crystals. *Source:* © Kurt Hollochern Geology Dept, Union College, NY. (See electronic version for color figures)

role of electron donor and acceptor, respectively [21]. The deep-brown to black color of these glasses is an interesting visual proof for clustering of transition element in glasses with a significant covalent bonding in and between the Fe sites.

During lunar exploration, an original 3.48-billion-year-old orange glass has been found near a small crater at the Apollo 17 landing site (Figure 13). This glass color comes from a Fe^{2+} (donor)–O^{2-}–Ti^{4+} (acceptor) charge-transfer transition near 24 000 cm^{-1}. Synthetic glasses containing Fe or Ti and synthesized under simulated reducing lunar conditions exhibit a green or a purple color, respectively. It is only the association between the two transition elements that results in this original color [19]. This fact provides further proof of the heterogeneous distribution of transition element cations in glass structure, favoring a location in specific enriched regions. Similar Fe–Ti IVCT may be used for enhancing UV absorption in container glasses for drugs and cosmetics.

7 Absorption by Organized Clusters and Nanophases

7.1 Presence of Organized Clusters: Low-Alkali Borate and Borosilicate Glasses

Nickel- and cobalt-bearing alkali-poor borate glasses exhibit original green and light pinkish purple colorations, respectively. Similar colors are found in borosilicate [6] but not in silicate glasses. For decades, these features have been assigned to the presence of Ni and Co in octahedral sites within the glass structure. More recently, Ni- and Co–K edge EXAFS data on these glasses have revealed cation–cation correlations up to 6 Å in ordered NiO- or CoO-based clusters and characterized by three colinear, edge-sharing octahedra, which induce a specific multiple scattering feature around 6 Å. Some structural features characteristic of the bulk oxides (CoO or NiO) are missing, however, showing that these ordered domains do not correspond to pure oxide crystallites [2]. This environment is not affected by Ni or Co concentration and disappears with increasing alkali content.

The presence of similarly ordered domains in low-alkali borosilicate glasses shows that $^{[6]}$Ni (and probably $^{[6]}$Co) is preferentially associated with a borate rather than with a silicate sublattice. This local coordination is likely favored by the geometrical constraints induced by the presence of rigid large $^{[3]}$B-based superunits. But the EXAFS data indicate a less extended structural order in the NiO nanodomains, probably due to the mutual interaction between borate and silicate sublattices, which limits their extent [6].

7.2 Metallic Nanoparticles

Although *Ruby* glasses have been known for centuries (e.g. the famous fourth-century Lycurgus cup), their deep ruby-red or yellow colors have been explained only

recently in terms of precipitation of Au, Cu, or Ag nanoparticles 5–100 nm in diameter [22]. These nanoparticles form during thermal treatments above the annealing temperature of colorless starting glasses prepared under reducing conditions such that the dilute (40–300 ppm) coloring metal ion is present in its reduced form (e.g. Au^{+}). Gold reduction has been accomplished historically by using Sn as a reducing agent, following the reaction:

$$Sn^{2+} + 2\,Au^{+} \rightarrow Sn^{4+} + 2\,Au^{0} \qquad (7)$$

However, the electrons needed for gold reduction may be provided by other redox reactions and even from external irradiation. The ruby-red color of the gold nanoparticles is due to a resonant absorption of photons during the excitation of surface plasmons within the nanoparticles. It is a typical example of quantum (electron) confinement effects observed when crystallites are smaller than the wavefunction of an electronic state. This color is often referred to as *striking* because it suddenly appears upon heating.

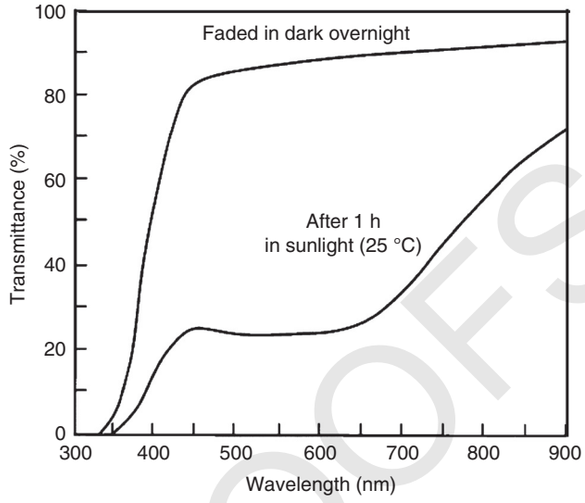

Figure 14 Transmittance curves for the crown glass used for Photogray Extra® photochromic lens in its lightened (faded) and darkened states. *Source:* After [23].

7.3 Photochromic Glasses

Photochromic glasses darken or change color when exposed to light or UV radiation, giving rise to a wide range of applications such as ophthalmic lenses, architectural or automotive glazing, information storage, and display devices [23]. A phenomenon that has found important practical applications in optics relies on the presence of silver halide particles of a few nm precipitated in the glass through an appropriate heat treatment. When the glass is exposed to near-UV visible light, a dark coloration rapidly appears but the glass lightens more slowly when returned to the dark. It is interesting that generally the glasses do not darken completely inside a car, because the car windows block some of the UV radiation needed for the photochromic reaction. Temperature effects are intriguing: the higher the temperature, the less dark photochromic glasses will be, as, conversely, photochromic glasses will take longer to regain their transparency under low ambient temperature.

Under exposure to light, Ag^{+} is reduced into Ag^{0}, the halogen ions acting as the reducing agent providing electrons for silver particle formation. This results in light absorption by the conduction electrons of metallic Ag over the entire visible range, giving a neutral coloration (Figure 14). Some sensitizers such as Cu^{+} may be added to speed up the process, which act as an electron donor for Ag^{+}. The limited diffusion of halogens in the glass at room temperature is at the origin of the reversibility of the process, needed by most uses of photochromic glasses. Halogens serve as sinks for electrons as Ag oxidation proceeds during the fading stage.

8 Perspectives

Light absorption by colored glasses remains an area that has great potential for development in many fields. Conversely, there is a continuous interest in ultrawhite glass for solar energy and data transmission applications, with the necessity to model the parasitic absorption caused by absorbing centers. The ability to modify the speciation of transition metal ions by modifying glass composition or melting conditions is an important advantage of glasses over crystalline matrices. The chemical dependence of the structure of oxide glasses, wherein transition metal ions occupy a large diversity of sites, opens the way for selecting specific environments that will impart original coloration. The chemical dependence of the geometry and relative proportion of the sites occupied by transition metal ions may sometimes be combined with an adjustment of the oxidation states as a function of synthesis conditions. This unique feature will continue to open the way to novel colors in glass materials.

Finally, regarding historical and cultural aspects (Ch. 10.6, 10.8), spectroscopic analyses may be used to improve our knowledge of ancient glassmaking technologies. Non-invasive portable spectrometers give information on the speciation of transition elements. The investigation of stained glasses from the 12th–13th centuries, which are blue colored by tetrahedral Co^{2+}, shows that more reducing conditions were achieved in medieval than in modern furnaces, enhancing the blue color by favoring Fe as Fe**2+** and Cu and Mn as non-coloring

Cu^{+} or weakly coloring Mn^{2+}, respectively [23]. The colorimetric analysis of stained glasses confirms the skills of medieval glassmakers to master redox kinetics and develop innovative glass colors.

References

1 Weyl, W.A. (1967). *Colored Glasses*. Sheffield: Society of Glass Technology.

2 Calas, G., Cormier, L., Galoisy, L., and Jollivet, P. (2002). Structure-property relationships in multicomponent oxide glasses. *C. R. Chim.* 5: 831–843.

3 Calas, G., Galoisy, L., Cormier, L., and Lefrère, Y. (2006). La couleur des verres: le rôle des éléments de transition. *Verre* 12: 5–11.

4 Burns, R.G. (1993). *Mineralogical Applications of Crystal Field Theory*. Cambridge: Cambridge University Press.

5 Galoisy, L. (2006). Structure–property relationships in industrial and natural glasses. *Elements* 2: 293–297.

6 Galoisy, L., Calas, G., Cormier, L. et al. (2005). Overview of the environment of Ni in oxide glasses and relation with the glass coloration. *Phys. Chem. Glasses* 46: 394–399.

7 Jackson, W.E., Farges, F., Yeager, M. et al. (2005). Multi-spectroscopic study of Fe(II) in silicate glasses: implications for the coordination environment of Fe(II) in silicate melts. *Geochim. Cosmochim. Acta* 69: 4315–4332.

8 Bingham, P.A., Hannant, O.M., Reeves-McLaren, N. et al. (2014). Selective behaviour of dilute Fe^{3+} ions in silicate glasses: an Fe K-edge EXAFS and XANES study. *J. Non Cryst. Solids* 387: 47–56.

9 Villain, O., Galoisy, L., and Calas, G. (2010). Spectroscopic and structural properties of Cr^{3+} in silicate glasses. *J. Non Cryst. Solids* 356: 2228–2234.

10 Hunault, M., Calas, G., Galoisy, L. et al. (2014). Local ordering around tetrahedral Co^{2+} in silicate glasses. *J. Am. Ceram. Soc.* 97: 60–62.

11 Calas, G., Majérus, O., Galoisy, L., and Cormier, L. (2006). Crystal field spectroscopy of Cr^{3+} in glasses: compositional dependence and thermal site expansion. *Chem. Geol.* 229: 218–226.
Calas, G., Majérus, O., Galoisy, L., and Cormier, L. (2006). Crystal field spectroscopy of Cr^{3+} in glasses. *Chem. Geol.* 229: 218–226.

12 Chopinet, M.H., Lizarazu, D., and Rocanière, C. (2002). L'importance des phénomènes d'oxydo-réduction dans le verre. *C. R. Chim.* 5: 939–949.

13 Villain, O., Calas, G., Galoisy, L. et al. (2007). XANES determination of chromium oxidation states in glasses: comparison with optical absorption spectroscopy. *J. Amer. Ceram. Soc.* 90: 3578–3581.

14 Lin, T. and Angell, C.A. (1984). Electronic spectra and coordination of Ni^{2+} in potassium borate glass and melt to 1000°C. *J. Am. Ceram. Soc.* 67: C33–C34.

15 Möncke, D., Ehrt, D., Eckert, H., and Mertens, V. (2003). Influence of melting and annealing conditions on the structure of borosilicate glasses. *Phys. Chem. Glasses* 44: 113–116.

16 Glebov, L.B. and Boulos, E.N. (1998). Absorption of iron and water in the Na_2O-CaO-MgO-SiO_2 glasses. II. Selection of intrinsic, ferric, and ferrous spectra in the visible and UV regions. *J. Non Cryst. Solids* 42: 49–62.

17 Efimov, A.M., Ignatiev, A.I., Nikonorova, N.V., and Postnikov, E.S. (2013). Quantitative UV–VIS spectroscopic studies of photo-thermo-refractive glasses. II. Manifestations of Ce^{3+} and Ce(IV) valence states in the UV absorption spectrum of cerium-doped photo-thermo-refractive matrix glasses. *J. Non Cryst. Solids* 361: 26–37.

18 Nolet, D.A. (1980). Optical absorption and Mössbauer spectra of Fe, Ti silicate glasses. *J. Non Cryst. Solids* 37: 99–110.

19 Koepke, C., Wisniewski, K., and Grinberg, M. (2002). Excited state spectroscopy of chromium ions in various valence states in glasses. *J. Alloys Compd.* 341: 19–27.

20 Bingham, P.A., Parker, J.M., Searle, T. et al. (1999). Redox and clustering of iron in silicate glasses. *J. Non Cryst. Solids* 253: 203–209.

21 Ravel, B., Carr, G.L., Hauzenberger, C.A., and Klysubun, W. (2015). X-ray and optical spectroscopic study of the coloration of red glass used in 19th century decorative mosaics at the Temple of the emerald Buddha. *J. Cult. Herit.* 16: 315–321.

22 G.L. Stephens and J.K. Davis, Duane's ophthalmology, Ch. 51D *Ophthalmic Lens Tints and Coatings*, Lippincott Williams & Wilkins: Philadelphia (2006) http://www.oculist.net/downaton502/prof/ebook/duanes/pages/v1/v1c051d.html (accessed 27 May 2020).

23 Hunault, M., Bauchau, F., Loisel, C. et al. (2016). Spectroscopic investigation of the coloration and fabrication conditions of medieval blue glasses. *J. Am. Ceram. Soc.* 97: 60–62.